Inorganic Chemistry

ARTICLE

pubs.acs.org/IC

Nearest- and Next-Nearest-Neighbor Ru(II)/Ru(III) Electronic Coupling in Cyanide-Bridged Tetra-Ruthenium Square Complexes.

Ju-Ling Lin,[†] Chia-Nung Tsai,[†] Sheng-Yi Huang,[†] John F. Endicott,[*,‡] Yuan-Jang Chen,[*,†] and Hsing-Yin Chen[§]

[†]Department of Chemistry, Fu-Jen Catholic University, New Taipei City 24205, Taiwan, R.O.C.

[‡]Department of Chemistry, Wayne State University, Detroit, Michigan 48202, United States

[§]Department of Medicinal and Applied Chemistry, Kaohsuing Medical University, Kaohsuing 807, Taiwan, R.O.C.

Supporting Information

ABSTRACT: Electrochemical properties of cyanide-bridged metal squares, $[Ru_4]^{4+}$ and $[Rh_2{-}Ru_2]^{6+}$, clearly demonstrate the role of the nearest (NN) metal moiety in mediating the next-nearest neighbor (NNN) metal-to-metal electronic coupling. The differences in electrochemical potentials for successive oxidations of equivalent Ru(II) centers in $[Ru_4]^{4+}$ are $\Delta E_{1/2}$ = 217 mV and 256 mV and are related to intense, dual metal-to-metal-charge-transfer (MMCT) absorption bands. This contrasts with a small value of $\Delta E_{1/2}$ = 77 mV and no MMCT absorption bands observed to accompany the oxidations of $[Rh_2{-}Ru_2]^{6+}$. These observations demonstrate NN-mediated superexchange mixing by the linker Ru of NNN Ru(II) and Ru(III) moieties and that this mixing results in a NNN contribution to the ground state stabilization energy of about 90 ± 20 meV. In contrast, the classical Hush model for mixed valence complexes with the observed MMCT absorption parameters predicts a NNN stabilization energy of about 6 meV. The observations also indicate that the amount of charge delocalization per Ru(II)/Ru(III) pair is about 4 times greater for the NN than the NNN couples in these CN-bridged complexes, which is consistent with DFT modeling. A simple fourth-order secular determinant model is used to describe the effects of donor/acceptor mixing in these complexes.

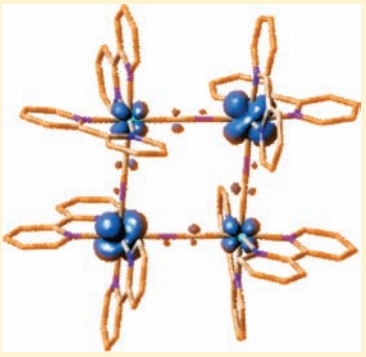

INTRODUCTION

The electronic properties of complexes with an approximately square cyanide-bridged tetrametallic core have been of some interest recently.[1−7] When the metals can be oxidized or reduced, the electronic mixing between metals in different formal oxidation states can in principle lead to delocalization of charge density in the mixed valence species generated, and this delocalization can alter the physical and chemical properties of the complexes.[8−17] However, it is generally difficult to evaluate the extent of electronic delocalization between the metal centers in these systems since (a) the best developed descriptions of mixed valence complexes were obtained for the weak coupling limit in which the delocalization is very small[8−10,12,14] and (b) most of these approaches are based on the properties of metal to metal charge transfer (MMCT) absorption bands, and the orbital compositions of the observed transitions are rarely well established for the electron-rich metals that are often used in such studies. Furthermore, electroabsorption studies have shown that the weak coupling approach can greatly underestimate the donor−acceptor (D/A) mixing in complexes with large mixing matrix elements.[18−21]

The cyanide linkage of D/A pairs of metals can be "non-innocent", and it can contribute to a variety of complex properties even when there is a significant difference in the potentials for oxidizing and reducing the complexes and the D/A mixing is relatively weak.[22,23] When the difference between the donor oxidation and acceptor reduction potentials, $F\Delta E_{1/2}$ (F is Faraday's constant), is small, much greater D/A mixing is expected, and there should be corresponding alterations in complex properties. Multimetallic complexes with the metals bridged by cyanide differ from their analogs with polypyridyl bridging ligands (such as pyrazine) in the high energies of their metal to or from cyanide charge transfer (MLCT or LMCT, respectively) absorptions.[23] As a consequence, the effects of D/A mixing between next nearest neighbor metals tend to be interpreted in terms of the mediation by the intermediate metal center rather than by the cyanide.[1] This approximation either ignores the contributions of the bridging cyanide or assumes that some molecular orbital of the intermediate $(L)M(CN)_2$ linker mediates the mixing of the remote metals. While it is difficult to evaluate the validity of this assumption, it does point to a unique feature of the cyanide-bridged complexes.

The D/A couples generated by one-electron oxidation of the simple CN-bridged tetra-metallic square complexes reported in this study are linked by two $(L)M(CN)_2$ moieties, and this amplifies the effects of NN mediated NNN mixing, thereby providing some unique insights into the issues related to strong D/A mixing.

Received: April 19, 2011
Published: August 02, 2011

EXPERIMENTAL SECTION

1. Materials and Synthesis of Compounds. The following commercial chemicals were used with no further purification: $RuCl_3 \cdot 3H_2O$, $Ru(bpy)_2Cl_2 \cdot 2H_2O$, and NH_4PF_6 (STREM); $RhCl_3 \cdot 3H_2O$ (KOJUNDO); 2,2′-bipyridine, 2,2′:6′,3″-terpyridine, and trifluoromethanesulfonic acid-*d* (DOTF) (Aldrich); and KPF_6 (SHOWA). The syntheses of the following compounds have been reported elsewhere: *cis*-$[Ru(bpy)_2(CN)_2](H_2O)_2$,[24] *cis*-$[Rh(bpy)_2Cl_2](PF_6)$,[25] *cis*-$[Rh(bpy)_2(CN)_2](PF_6)$,[26] and $[(bpy)_2Ru\{CNRu(tpy)(bpy)\}_2](PF_6)_4$.[27]

[Ru₄](PF₆)₄. A mixture of 49.65 mg (0.095 mmol) of $[Ru(bpy)_2Cl_2]$-$(H_2O)_2$ and 50.10 mg (0.100 mmol) of $[Ru(bpy)_2(CN)_2](H_2O)_2$ in 31 mL of H_2O was refluxed for 4 days. Then, 2 mL of saturated aqueous NH_4PF_6 solution was injected into a round-bottom flask, and the mixture was chilled to precipitate the target complex, $[Ru_4](PF_6)_4$. All steps of the synthesis were carried out in an argon atmosphere. The sample was chromatographically purified twice (with aluminum oxide 90 active neutral, purchased from Merck, as the stationary phase, and a 1:3 (v/v) mixture of CH_3CN and toluene as the eluent). The second brown band contained the desired compound. The solvent was removed by rotary evaporation followed by drying in a vacuum. The typical yield was 82%. Anal. Calcd (found) for $C_{84}H_{64}N_{20}F_{24}P_4Ru_4$: C, 43.16 (42.69); H, 2.76 (2.82); N, 11.98 (12.05).

[Rh₂Ru₂](PF₆)₆·(H₂O)₄. This reaction was carried out in an argon atmosphere. A solution containing 101.62 mg (0.166 mol) of $[Rh(bpy)_2(CN)_2](PF_6)$, 86.93 mg (0.167 mmol) of $Ru(bpy)_2Cl_2 \cdot 2H_2O$, and 20 mL of a 1:1 (v/v) mixture of ethylene glycol/H_2O was refluxed for 4 days. A saturated aqueous solution of KPF_6 (3 mL) was added to the solution, the mixture was cooled to room temperature, and the crude product was removed by filtration. The crude product was purified by chromatography using the above procedure. The typical yield of the bright red-orange product was 18%. Anal. Calcd (found) for $C_{84}H_{72}N_{20}F_{36}O_4P_6Rh_2Ru_2$: C, 37.32 (37.07); H, 2.68 (2.45); N, 10.36 (10.52).

Electrochemistry. Electrochemical measurements were performed using an Epsilon Electrochemical Workstation. Cyclic voltammograms (CV) and differential pulse voltammograms (DPV) were obtained in acetonitrile solution, which contained 10^{-3} M complex and 0.1 M *n*-tetrabutylammonium hexafluorophosphate (*n*-TBAH) at scan rates of 100 mV/s and 4 mV/s, respectively. A three-electrode system consisting of a Pt disk (1 mm) as a working electrode, polished with 0.1−0.3 μm Baikowski alumina suspension, a Pt wire as the counter electrode, and Ag/AgCl as the reference electrode was used. Ferrocene (0.437 V vs Ag/AgCl) was used as the internal standard.

Absorption Spectroscopy (UV−vis−NIR). UV−vis−NIR absorption spectra of these multimetal complexes in a solution of CH_3CN/H_2O = 1:1 (v/v) were determined with a Shimadzu UV-3101PC spectrophotometer at 298 K. The spectral changes that accompanied redox titrations were obtained with the target complexes dissolved in the [DOTF] = 0.03 M solution (CH_3CN/D_2O = 1:1 (v/v)) and 3×10^{-3} M $(NH_3)_2Ce(NO_3)_6$, as the oxidant, or 1.5×10^{-3} M ferrocene, as the reductant; the CH_3CN/D_2O = 1: 1 (v/v) solutions of both oxidant and reductant contained 0.03 M [DOTF].

Computational Methods. Density functional theory (DFT) calculations with the Becke three-parameter hybrid functional B3LYP[28] were used in this work. The atoms were represented with the LANL2DZ[28−30] basis set implemented in the Gaussian 03 program.[31] For $[Ru_4]^{5+/6+}$, only C_2 constrained geometry optimizations were performed. Since all of the calculated electronic states were open-shell, spin-unrestricted wave functions were employed. The properties of electronically excited states were calculated by the time-dependent DFT (TD-DFT) approach with the Gaussian 03 package.[31] The UV-vis absorption spectra were simulated by using the data of TD-DFT calculations with full width at half-height of 2000 cm^{-1}; this was achieved by using the GaussView program.[32] The calculated low-energy absorption spectra, the composition of electronic transitions, the associated molecular orbitals, and the Mulliken spin densities and charges for the series of mixed-valence complexes are shown in the Supporting Information S1.

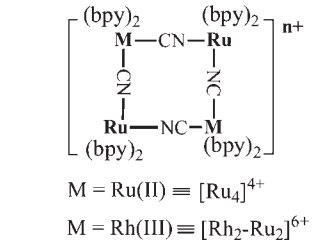

Figure 1. Schematic representations of the square complexes. Since the M and Ru sites differ in their linkage to cyanide, they will be distinguished as M_C, $M_{C'}$, Ru_N, and $Ru_{N'}$.

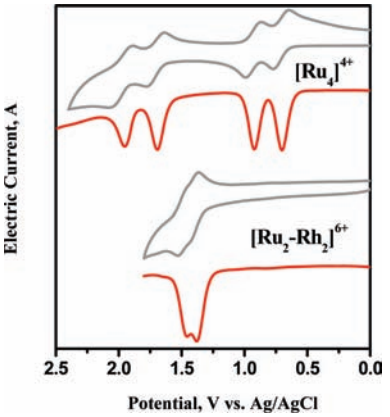

Figure 2. The cyclic voltammograms (gray curves) and differential pulse voltammograms (red curves) of $[Rh_2{-}Ru_2]^{6+}$ and $[Ru_4]^{4+}$ vs Ag/AgCl in acetonitrile with 0.1 M TBAH.

RESULTS

In this work, we have synthesized the square complexes $[Ru_4]^{4+}$ and $[Rh_2{-}Ru_2]^{4+}$, in which $Ru(II)(bpy)_2$ moieties are linked by cyanide, see Figure 1. The oxidations of the chemically equivalent $Ru(II)(bpy)_2$ moieties of the former occur in well separated, electrochemically distinct steps, as shown in Figure 2, and they result in the low energy metal-to-metal charge transfer absorptions, which are shown in Figure 3 and summarized in Table 1. In contrast, the electrochemical oxidations of the $[Rh_2{-}Ru_2]^{6+}$ complex are not as well separated, and we have not detected any absorption changes at energies less than 15 000 cm^{-1} accompanying the oxidations. These electrochemical observations are clear evidence for the mediation of next nearest neighbor (NNN) Ru(II) and Ru(III) superexchange[12,14] mixing by the nearest neighbor (NN) $(bpy)_2Ru(CN)_2$ linker, and this is discussed in detail below.

The DFT modeling of the $[Ru_4]^{5+}$ complex[38] results in the same spin and, by inference, charge densities on NNN metals, and this is not consistent with the unsymmetrical distribution of charge (about 90% on Ru_N and about 10% on $Ru_{N'}$) implicated by the electrochemical observations on the doubly bridged NNN metals (see the Discussion section).[38] It is possible that this is a problem of a tendency of the DFT approach to give symmetrical

dx.doi.org/10.1021/ic200806a |*Inorg. Chem.* 2011, 50, 8274–8280

charge distributions in chemically equivalent moieties[39] within a molecule, and this is being further investigated. In contrast, the DFT calculations on the $[Ru_4]^{6+}$ complex indicate about 16% charge delocalization between NN Ru centers, which is consistent with the inferences from the electrochemical measurements.

DISCUSSION

The absorption spectra of linked D/A complexes have traditionally been interpreted in terms of models that assume single donor and acceptor orbitals that are weakly mixed.[11,14,15,40,41] Such models are of limited value for electron-rich donors such as Ru(II), which have several potential donor orbitals that are similar in energy, and when the D/A mixing is very strong. Thus, each Ru center in the complexes considered here contains three dπ orbitals that do not differ much in energy, so that the orbital compositions of the observed absorption bands are often ambiguous. As a consequence, the experimental assessment of D/A mixing is much more straightforward when based on the electrochemical properties of the relatively simple square complexes with cyanide-bridged $Ru^{III,II}(bpy)_2$ D/A moieties, and it demonstrates that there is much more electronic mixing between the remote centers than inferred from the weak mixing models.

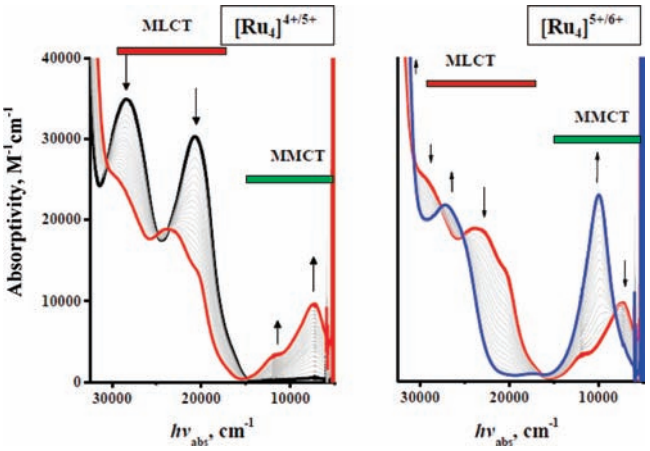

Figure 3. Absorption changes that accompany Ce^{4+} oxidations of the Ru centers of the −CN-bridged complex, $[Ru_4]^{4+}$: black curve, $[Ru_4]^{4+}$; red curve, $[Ru_4]^{5+}$; and blue curve, $[Ru_4]^{6+}$.

The DFT modeling of the absorption spectra of the complexes reported here and for some related Ru-polypyridyl complexes discussed previously[42,43] indicates that the dominant observed absorption bands are often the convolution of several components that differ in their orbital composition and that the HOMO−LUMO transitions, which generally correlate with the oxidation/reduction properties of the complexes, are often difficult to identify due to small oscillator strengths and/or very low energies.[27,43] This is particularly a concern in the class of complexes considered here because the NN $Ru(bpy)_2$ centers differ only in their linkage to cyanide, and this should result in small intrinsic values of $F\Delta E_{1/2}$ while the electron-transfer reorganizational energies of the $Ru(bpy)_2$ moieties are also expected to be relatively small.[17] As a result, there could be very low energy MMCT transitions. Such a low energy absorption band ($\sim$4000 cm^{-1}) has been reported to result from oxidation of the closely related $[Fe_4]^{4+}$ complex.[6]

There are fewer ambiguities in the interpretation of our electrochemical observations. Thus, the lowest energy Rh(III) acceptor orbitals occur at such high energies that the NN Ru(II)/Rh(III) mixing is effectively zero in $[Rh_2-Ru_2]^{6+}$, and a very small value of $\Delta E_{1/2}$ = 77 meV is observed for oxidations of the chemically equivalent Ru(II) centers. The sum of contributions from through space Ru(II)/Ru(III) mixing, ε^{tp}_{NNN}, and several electrostatic factors[37] that accompany the NNN oxidation, ε^{el}_{NNN}, are approximately 77 meV. However, the differences in solvating oxidized and reduced species are expected to dominate ε^{el}_{NNN}, and replacing Rh(III) by Ru(III), which should not alter (ε^{tp}_{NNN} + ε^{el}_{NNN}), increases $\Delta E_{1/2}$ by 180 mV. This increase can be attributed to twice the stabilization energy that results from NN Ru(III) mediation of NNN Ru(II)/Ru(III) coupling, $2\varepsilon^{spx}_{NNN}$, in the $[Ru_4]^{7+}$ complex. Since there are two bridging linkages in the $[Ru_4]^{7+}$ complex, this implies a superexchange contribution of ε^{spx}_{NNN}/(bridging unit) $\approx$ 45 meV ($\approx$ 360 cm^{-1}); if the contributions are approximately additive, this corresponds to the NNN stabilization energy in the comparable trimetallic

Table 1. MMCT Absorption and Electrochemical Parameters of Some Mixed-Valence Multi-Metal Ions

	$E_{1/2}$(Ru(III/II))		$F\Delta E_{1/2}$		MMCT absorption parameters		
complexes[a]	charge (n+) range	V (DPV) [b]	eV	cm^{-1}	charge (n+)	hν_{max}(low) ($\varepsilon/10^3$) [$\Delta\nu_{1/2}$] [c]	hν_{max}(high) ($\varepsilon/10^3$) [$\Delta\nu_{1/2}$] [c]
$[Ru_4]^{n+}$	(4+) to (6+)	0.717, 0.930 (0.692, 0.909)	217	1750	5+	7.47 (9.6)[3.4]	11.6 (3.4) [3.4]
	(6+) to (8+)	1.687, 1.970 (1.680, 1.936)	256	2060	6+	10.0 (23.0)[3.3] [d]	
$[Rh_2-Ru_2]^{n+}$	(6+) to (8+)	1.449 (1.379, 1.456)	77	620	[all]	(ε < 200 M^{-1} cm^{-1} between 10000 and 15000 cm^{-1})	
cis-$[Ru(bpy)_2\{CN\text{-}Ru(bpy)(tpy)\}_2]^{n+}$ [d]	(4+) to (6+)	1.008, 1.137 (0.983, 1.117)	129	1040	5+	7.63 (5.8) [4.0]	10.6 (1.4) [3.8]
	(6+) to (7+)	1.820			6+	8.90 (8.4) [4.4]	
cis-$[Ru(bpy)_2\{CN\text{-}RuA_5\}_2]^{n+}$ [e,f]	(4+) to (6+)	0.055, 0.125	70	560	5+	9.5 (0.35) [4.2]	14.6 (3.3)[4.4]
	(6+) to (7+)				6+		15.3 (6.0)[5.7]
trans-$[(Am)_4Cr(CNRuA_5)_2]^{n+}$ [f,g]	(5+) to (7+)	0.36			6+	10.0 (0.14) [5.1] [h]	20.0 (8) [4.9]

[a] This work except as indicated. [b] Cyclic voltammograms of 0.1 M TBAH/CH_3CN with a Ag/AgCl reference electrode and ferrocene ($E_{1/2}$ = 0.437 V vs Ag/AgCl) as an internal reference except as indicated. ν_{max} = absorption maxima in $cm^{-1}/10^3$; ε = molar absorptivity, $M^{-1}cm^{-1}$; $\Delta\nu_{1/2}$ = full bandwidth at half height in $cm^{-1}/10^3$; E_{MMCT} = fitted Gaussian-maximum; in 0.03 M aqueous DOTF ([DOTF] = 0.03 M, except as indicated. [c] Absorption spectra in mixed solvents (D_2O/CH_3CN, v/v = 1/1; in this work). [d] Data from ref 22 [e] References 23 and 33. [f] A = NH_3. [g] References 34−36; Am = 1,4,7,10-tetraazacyclotetradecane. [h] Based on spectral changes resulting from incremental Ce(IV) oxidations of the fully reduced complex in deaerated 0.1 M aqueous $NaHSO_4$ solutions with the absorbance maximum evaluated from a Job's plot described in ref 37.

dx.doi.org/10.1021/ic200806a |Inorg. Chem. 2011, 50, 8274–8280

complex. Although the contributions of ε^{tp}_{NNN} are probably comparable, ε^{el}_{NNN} is likely to be smaller for the first two oxidations of $[Ru_4]^{4+}$, so by using $(\varepsilon^{tp}_{NNN} + \varepsilon^{el}_{NNN}) \approx 77$ meV and allowing for an experimental uncertainty of ± 5 mV in each electrochemical determination we obtain, reasoning as above, $64 > \varepsilon^{spx}_{NNN}/\text{meV} \geq 35$ per bridging unit in the $[Ru_4]^{5+}$ complex. Thus, the estimates of ε^{spx}_{NNN} for the two NNN Ru(II)/Ru(III) couples are small and comparable, with ε^{spx}_{NNN}/bridging unit $\approx 45 \pm 10$ meV. Similarly, we find $47 > \varepsilon^{spx}_{NNN}/\text{meV} \geq 30$ in the trimetallic $[Ru(CN{-}Ru)_2]^{4+}$ complex (with one bridging unit); this is based on the assumption that $(\varepsilon^{tp}_{NNN} + \varepsilon^{el}_{NNN}) \approx 35{-}70$ meV since the oxidations of equivalent Ru(tpy)(bpy) moieties of $[Ru(CN\text{-}Ru)_2]^{4+}$ were indistinguishable.[27] These electrochemistry-based observations put significant constraints on the magnitude of the NN mixing.

The relationship between the NN D/A mixing and the NN mediated NNN D/A mixing is commonly classified as "superexchange" (spx), and it is usually formulated in terms of a three-state LCAO-based model:[12,14,44] donor (D), acceptor (A), and bridging ligand states (NN). This approach assumes that the NN and NNN mixings can be uniquely identified, for example, as expressed in terms of their respective stabilization energy contributions to the total ground state stabilization energy, $\varepsilon_{g(3)}$ (for a three-state model), that results from configurational mixing:

$$\varepsilon_{g(3)} \approx \varepsilon_{NN} + \varepsilon_{NNN} \quad (1)$$

Equation 1 is expressed as a sum of distinct mixing perturbations which are based on the respective diabatic energies so that $\varepsilon_{NN} = (H_{NN})^2/[E_{NN}(1 + (H_{NN}/E_{NN})^2)]$ and $\varepsilon_{NNN} = (H_{NNN})^2/[E_{NNN}(1 + (H_{NNN}/E_{NNN})^2)]$. If one assumes that ε_{NNN} is a linear combination of through space (tp) and bridging ligand mediated contributions, then a LCAO formalism leads to eq 2 with the limit that $\alpha^2_{NN} \ll \sim 0.1$.[12,14]

$$H^{spx}_{NNN} \approx \frac{H^2_{NN}(2E_{NN} - E_{NNN})}{2E_{NN}(E_{NN} - E_{NNN})} \quad (2)$$

Equation 2 has singularities for the diabatic energies at $E_{NN} = E_{NNN}$ and at $E_{NN} = 0$. Figure 3 suggests that $E_{NN} \sim E_{NNN}$ for $[Ru_4]^{5+}$ and that the NN mixing matrix elements are quite large so that substantial errors would be expected if this equation were used (see Figure 4). Alternatively, one can use the third order secular determinant, to represent perturbational mixing in the three state system, but this raises some issues regarding the definition of "superexchange" mixing. The simplest definition is the difference between the stabilization energy of a mixed valent three center system of the $D_tA_cA_{t'}$ (subscripts t and t′ for terminal and c for central) type from that for the equivalent two center system, so that $\varepsilon_{NNN} \approx \varepsilon_{g(3)} - \varepsilon_{g(2)}$. This definition differs somewhat from that in the weak coupling limit since some of the additional stabilization energy of a three center system can arise from an appreciable redistribution of charge among D_t, A_c, and $A_{t'}$ when $\alpha_{DA}{}^2 > 0.1$; however, it is reasonably straightforward and will be employed here.

In the weak coupling limit (for $\alpha_{NN}{}^2 \ll 0.1$), the spectroscopic parameters for the MMCT absorption can be related to the mixing matrix element by[8,9]

$$H_{NN} = \frac{0.0205}{r_{DA}}\sqrt{\varepsilon_{max}\Delta\nu_{1/2}\nu_{max(NN)}} \quad (3)$$

With the $h\nu_{max}$(low) parameters in Table 1 and $r_{DA} = 5.2$ Å (the distance between Ru(II) and Ru(III) centers), eq 3 results in

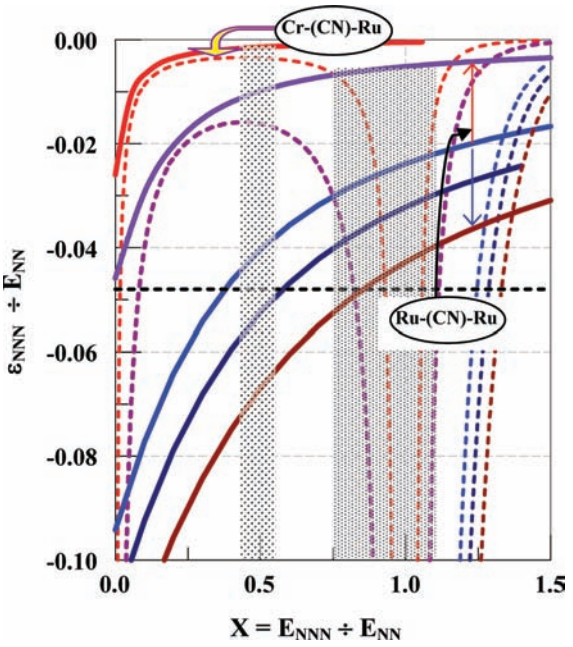

Figure 4. Comparison of perturbation theory models for contribution of a NNN center (e.g., $Ru_{N'}$) to the ground state stabilization, ε_g, per bridging moiety for different ratios of excited state energies. For $[Ru_4]^{5+}$, assuming $H^{(tp)}_{NNN} \approx 0$ and with $\alpha^2 = 0.25$, 0.2, 0.16, and 0.06 (dark red, dark blue, and purple curves, respectively): (a) with eigenvalues calculated using eq 4 for different ratios of $X = E_{NNN}/E_{NN}$ (solid curves) or (b) based on eqs 2 and 6 (dashed lines). Red curves for $[(Am)_4Cr(CNRu(NH_3)_5)_2]^{6+}$ ((Am)$_4$ = 1,4,7,7-tetraazacyclotetradecane (cyclam)) with $\alpha_{NN}{}^2 = 0.028$ (based on work in refs 23, 34, 36) and eigenvalues calculated from third order secular determinants (solid curves) or eq 2 (dashed lines). Note that the values of $\xi_{NNN} = \varepsilon_{NNN}/E_{NN}$ generated from eq 2 are less than -0.1 for $\alpha_{NN}{}^2 = 0.16$, 0.2, and 0.25 when $X < 1$. The gray rectangles correspond to plausible values of X for $[(Am)_4Cr(CNRu(NH_3)_5)_2]^{6+}$, left, and $[Ru_4]^{5+}$, right.

$H_{NN} \sim 1950$ cm^{-1} and $\alpha_{NN(H)}{}^2 \approx 0.07$. This value of $\alpha_{NN(H)}{}^2$ in eq 2 leads to $\varepsilon^{spx}_{NNN} \sim 27$ cm^{-1} (~ 3 meV) per bridging moiety, which is far smaller than the 360 cm^{-1} (45 meV) per bridging moiety that we observe. However, it is well documented[18,19,21] that inappropriately small values of H_{NN} are obtained from eq 3 based on the geometric distance between D and A centers and MMCT absorption spectra when the absorptivities are very large; such underestimates are usually attributed to overestimates of the effective dipole lengths of the optical transitions.

We have used a fourth order secular determinant, eq 4, to model the lowest energy eigenvalues for the ground state, ξ_G, for a $[Ru_4]^{n+}$, $\xi_G(Ru)$, and for a reference system, $\xi_G(ref)$,

$$\begin{vmatrix} 1-\xi & \alpha_{NN'} & \alpha_{NN} & 0 \\ \alpha_{NN'} & X-\xi & 0 & \alpha_{NN'} \\ \alpha_{NN} & 0 & -\xi & \alpha_{NN} \\ 0 & \alpha_{NN'} & \alpha_{NN} & 1-\xi \end{vmatrix} = 0 \quad (4)$$

All energies in eq 4 are relative to $E_{NN} = E_{NN}(Ru_N)$ so that $1 = E_{NN}/E_{NN}$, $\xi = \varepsilon/E_{NN}$, $\alpha_{NN} = H_{NN}/E_{NN}$, and $X = E_{NNN}/E_{NN}$. The distinction between α_{NN} and $\alpha_{NN'}$ is only for convenience in defining the reference model used: (a) for $[Ru_4]^{n+}$ $\alpha_{NN} = \alpha_{NN'}$; (b) for the equivalent reference system $\alpha_{NN'} = 0$. Then, the

dx.doi.org/10.1021/ic200806a |Inorg. Chem. 2011, 50, 8274–8280

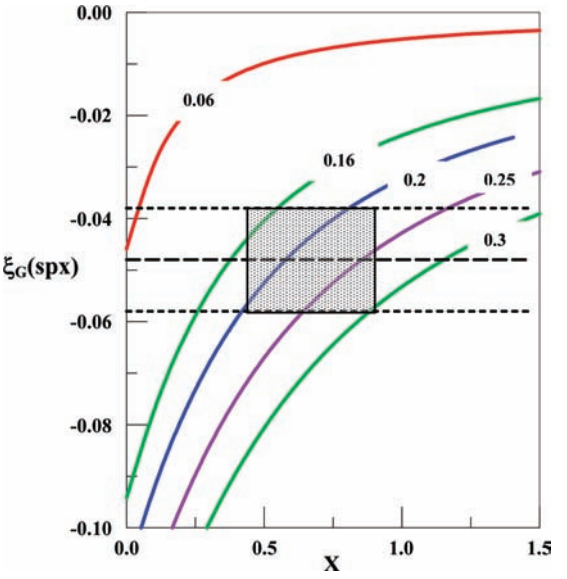

Figure 5. Reduced NNN superexchange energies calculated from the four-state model, eq 4, as a function of α_{NN}^2 and X. The values of α_{NN}^2 used are entered in the figure. The long dashed horizontal line is the value of $\xi_{NNN} = 0.048$ implied by the electrochemical observations, and the short dashed lines correspond to the estimated uncertainties in that value. The shaded box corresponds to the plausible range of values for X and α_{NN}^2.

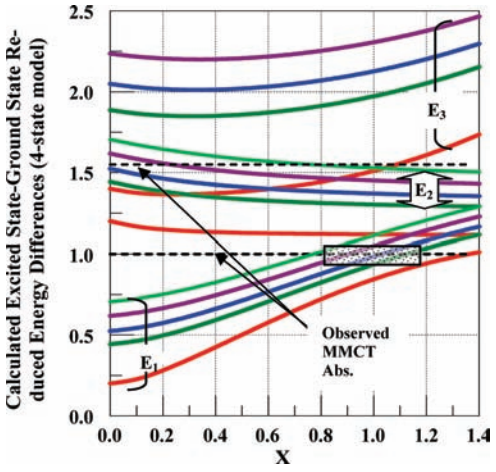

Figure 6. Energies of adiabatic MMCT excited states based on a four-state model (eq 4) in which the diabatic states are assumed to be pairs of degenerate states that differ in their reduced energy by 1.0. The curves are constructed for different values of α_{NN}^2 and X using the differences between the eigenvalues of eq 4 and relative to the ground state energy of 0: curve colors as in Figure 4. The shaded square indicates the plausible ranges of α_{NN}^2 and X.

lowest energy eigenvalues correspond to ξ_G(Ru) and ξ_G(ref), respectively, and the superexchange contribution is then

$$\xi_G(\text{spx}) = \xi_G(\text{Ru}) - \xi_G(\text{ref}) \quad (5)$$

For the comparisons in this paper, we have calculated values of the eigenvalues for increments 0.1 of $0 \leq X \leq 1.5$ (using PSI-Plot).[45]

For the comparison in Figure 3, we have used the reduced energies in eq 2 to define

$$\xi_G(\text{spxw}) = \varepsilon_{NNN}/E_{NN} = (H_{NNN}^{(spx)})^2/(E_{NNN}E_{NN}) = \left[\frac{\alpha_{NN}^2(2-X)}{2(1-X)}\right]^2\frac{1}{X} \quad (6)$$

In order to estimate plausible values of α_{NN}^2, we have calculated values of ξ_G(spx) for a range of values of X and α_{NN}^2 using eqs 4 and 5. The results are compared to the expectation based on the $[Ru_4]^{4+}$ electrochemistry in Figure 5, and they indicate that $\alpha_{NN}^2 = 0.20 \pm 0.05$ and $X = 0.90 \pm 0.15$.

This value of α_{NN}^2 combined with $E_{NN} = 7500$ cm^{-1} implies a (normalized) value of $H_{NN} \sim 3400$ cm^{-1}, which is similar to the value inferred previously from a variety of observations on the $[(bpy)_2Ru(CNRu(NH_3)_5)_2]^{5+}$ complex.[23]

The estimated values of α_{NN}^2 and X agree reasonably well with those based on the relative energies that are observed for the different MMCT transitions and those based on the eigenvalues of eq 4 as illustrated in Figure 6.

The relative values of ε_{NNN}^{spx} obtained using eq 2 and a third order secular determinant are reversed in their relative magnitudes for the $[(Am)_4Cr(CNRu(NH_3)_5)_2]^{6+}$ complexes examined by Watzky et al.[23] Thus, eq 3 and the NN spectroscopic parameters (and other observations)[23] give $H_{NN} \approx 3400$ cm^{-1} and $\alpha_{NN}^2 \sim 0.03$, so that eq 2 gives $H_{NNN} \sim 900$ cm^{-1} and $\varepsilon_{NNN}^{spx} = (H_{NNN})^2/E_{NNN} \approx 75$ cm^{-1}, but $\varepsilon_{NNN}^{spx} = 11$ cm^{-1} using the third order secular determinant with $X = 0.5$. These estimates of the superexchange stabilization energy for the Cr complex are both larger than the value of about 2.7 cm^{-1} implied by eq 3 and the observed MMCT spectral parameters.[23] Note that, even excluding those regions where singularities dominate eq 2, Figure 3 shows that the secular determinant-perturbation theory approach leads to smaller values of ε_{NNN}^{spx} than found using eq 2 and $\alpha_{NN}^2 > 0.03$ and that this difference decreases with α_{NN}^2. Although $\varepsilon_{NNN}^{spx} = 11$ cm^{-1}, based on a third-order secular determinant, is only about 4 times greater than that based on the observed spectra and eq 3, the observation that the values of ε_{NNN} are nearly identical for a series of $[(Am)_4M(CNRu(NH_3)_5)_2]^{6+}$ complexes with different metal centers (M = Cr(III), Co(III) and Rh(III)) and very different values of E_{NN} and α_{NN}^2 suggests that a different explanation is necessary, possibly a vibronic constraint as discussed previously.[23,36] In this sense, the $[Ru_4]^{5+}$ system is very similar to the *trans*-$[(py)_4Ru(CNRu(NH_3)_5)_2]^{5+}$ system in which $X \sim 1$ and configurational mixing between the electron-transfer excited states relaxes the constraints on NNN mixing.[35]

The mixing of diabatic states leads to small changes in state energies only when $\alpha_{DA}^2 \ll 0.1$. So, the use of observed spectroscopic parameters in eqs 2 and 3 in the evaluation of the properties of mixed valence complexes in this limit should only lead to small discrepancies except in the regions of the singularities illustrated in Figure 3. However, since α_{DA}^2 is much larger than this for the complexes considered here, the observed electronic energies can be very different from those of the diabatic limit. When this is the case, the use of the observed spectroscopic parameters and eqs 2 and 3 will necessarily result in large errors in the evaluation of mixed valence complex properties. Figure 5 illustrates the variations in the adiabatic energies of a four state system for several values of α_{DA}^2.

Of course, any simple perturbation theory model can provide only a general guide to the interpretation of multimetal electron-rich systems such as discussed here, since there are a large

number of electronic excited states that differ little in energy and the coupling between them will alter the model's predictions. For example, the successive oxidations of $[Ru_4]^{4+}$ result in shifts of the energies of absorption bands assigned to MLCT transitions, which suggests that some of these excited states also mix with the MMCT states thereby altering the energy relations.

The above arguments overlook some complications that are intrinsic to these mixed valence systems. The most notable of these is that our DFT modeling of this class of complexes indicates that there are appreciable bridging cyanide contributions to their HOMOs (Supporting Information S1).[38] This is at least partly a consequence of the strong oxidizing capacity of the $Ru(III)(bpy)_2$ centers, and the resulting delocalization of charge onto the bridging ligand must contribute to the observed stabilization energies, but this is very difficult to model in a simple manner. The second notable issue is the nature of the observed transitions. Figures 4 and 5 indicate that $0.8 < X < 1.2$ so that the observed absorption bands are likely to be mixtures of the NN and NNN MMCT transitions. However, Figure 5 also suggests that it is unlikely that there are relevant MMCT transitions at energies lower than about 5000 cm^{-1} in these complexes.

CONCLUSIONS

The $[Ru_4]^{4+}$ and $[Rh_2Ru_2]^{6+}$ square complexes discussed here are unique in that it is possible to estimate ground state superexchange stabilization energies of equivalent ruthenium centers based on well-defined and distinct electrochemical oxidations of $[Ru_4]^{2+}$ and from this to infer that $\alpha_{NN}^2 \sim 0.2$. This demonstrates much stronger Ru^{II}/Ru^{III} electronic mixing and greater electronic delocalization than is implied by the interpretation of the MMCT spectra using the conventional Hush treatment (eq 3). DFT modeling supports the inference of appreciable electronic delocalization in the mixed valence tetra-ruthenium complexes. The optical and electrochemical properties of these complexes illustrate how badly the conventional, superexchange treatment, eq 2, misrepresents the electronic coupling between a remote D/A pair when the energies of the diabatic MMCT and bridging ligand excited states are similar in energy and the donor/bridging ligand mixing is appreciable. A simple secular determinant approach for introducing the electronic perturbations has been shown to provide a much more reasonable description of the mixed valence systems.

ASSOCIATED CONTENT

Supporting Information. Computed MMCT absorption spectra, selected SOMO structures, Mulliken-densities of $[Ru_4]^{5+}$ and $[Ru_4]^{6+}$, and visible−ultraviolet region absorption spectra. This material is available free of charge via the Internet at http://pubs.acs.org.

AUTHOR INFORMATION

Corresponding Author

*E-mail: 054971@mail.fju.edu.tw (Y.-J.C.), jfe@chem.wayne.edu (J.F.E).

ACKNOWLEDGMENT

This work was funded in part (Y.-J.C.) by the National Science Council of R.O.C through Grants NSC-95-2113-M-030-003 and NSC-96-2113-M-030-006-MY2 and in part (J.F.E.) by the Division of Chemical Sciences, Geosciences, and Biosciences, Office of Basic Energy Sciences of the U.S. Department of Energy through Grant DE-FG02-09ER16120. We thank the National Center for High-Performance Computing (R.O.C.) for providing computational resources. We are grateful for many helpful comments and suggestions from Dr. R. L. Lord.

REFERENCES

(1) Newton, G. N.; Nihei, M.; Oshio, H. *Eur. J. Inorg. Chem.* **2011**, 3031.
(2) Nihei, M.; Sekine, Y.; Suganami, N.; Nakazawa, K.; Nakao, A.; Nakao, H.; Murakami, Y.; Oshio, H. *J. Am. Chem. Soc.* **2011**, *133*, 3592.
(3) Wang, S.; Ding, X.-H.; Zuo, J.-L.; You, X.-Z.; Huang, W. *Coord. Chem. Revs.* **2011**, *255*, 1713.
(4) Zueva, E. M.; Ryabikh, E. R.; Kuznetsov, A. M.; Borshch, S. A. *Inorg. Chem.* **2011**, *50*, 1905.
(5) Oshio, H.; Onodera, H.; Ito, T. *Chem.—Eur. J.* **2003**, *9*, 3946.
(6) Oshio, H.; Onodera, H.; Tamada, O.; Mizutani, H.; Hikichi, T.; Ito, T. *Chem.—Eur. J.* **2000**, *6*, 2523.
(7) Pardo, E.; Verdaguer, M.; Herson, P.; Rousseliere, H.; Cano, J.; Julve, M.; Lloret, F.; Lescouezec, R. *Inorg. Chem.* **2011**, *50*, 6250.
(8) Hush, N. S. *Prog. Inorg. Chem.* **1967**, *8*, 391.
(9) Hush, N. S. *Electrochim. Acta* **1968**, *13*, 1005.
(10) Hush, N. S. In *Mechanistic Aspects of Inorganic Reactions*; Rorabacher, D. B., Endicott, J. F., Eds.; ACS Symposium Series 198; American Chemical Society: Washington, DC, 1982; p 301.
(11) Creutz, C. *Prog. Inorg. Chem.* **1983**, *30*, 1.
(12) Newton, M. D. *Chem. Rev.* **1991**, *91*, 767.
(13) Meyer, T. J.; Taube, H. In *Comprehensive Coordination Chemistry*; Wilkinson, G., Gillard, R. D., McCleverty, J., Eds.; Pergamon: Oxford, England, 1987; Vol. 7, p 331.
(14) Creutz, C.; Newton, M. D.; Sutin, N. *J. Photochem. Photobiol. A: Chem.* **1994**, *82*, 47.
(15) Crutchley, R. *Adv. Inorg. Chem.* **1994**, *41*, 273.
(16) Barbara, P. F.; Meyer, T. J.; Ratner, M. *J. Phys. Chem.* **1996**, *100*, 13148.
(17) Endicott, J. F. In *Comprehensive Coordination Chemistry II*; 2nd ed.; McCleverty, J., Meyer, T. J., Eds.; Pergamon: Oxford, UK, 2003; Vol. 7, p 657.
(18) Oh, D. H.; Boxer, S. G. *J. Am. Chem. Soc.* **1990**, *112*, 8161.
(19) Brunschwig, B. S.; Creutz, C.; Sutin, N. *Coord. Chem. Rev.* **1998**, *177*, 61.
(20) Oh, D. H.; Sano, M.; Boxer, S. G. *J. Am. Chem. Soc.* **1991**, *113*, 6880.
(21) Shin, Y. K.; Brunschwig, B. S.; Creutz, C.; Sutin, N. *J. Phys. Chem.* **1996**, *100*, 8157.
(22) Macatangay, A. V.; Mazzetto, S. E.; Endicott, J. F. *Inorg. Chem.* **1999**, *38*, 5091.
(23) Watzky, M. A.; Macatangay, A. V.; Van Camp, R. A.; Mazzetto, S. E.; Song, X.; Endicott, J. F.; Buranda, T. *J. Phys. Chem. A* **1997**, *101*, 8441.
(24) Demas, J. N.; Turner, T. F.; Crosby, G. A. *Inorg. Chem.* **1969**, *8*, 674.
(25) Amarante, D.; Cherian, C.; Emmel, C.; Chen, H.-Y.; Dayal, S.; Koshy, M.; Megehee, E. G. *Inorg. Chim. Acta* **2005**, *358*, 2231.
(26) Endicott, J. F.; Song, X.; Watzky, M. A.; Buranda, T. *Chem. Phys.* **1993**, *176*, 427.
(27) Tsai, C.-N.; Allard, M. M.; Lord, R. L.; Luo, D.-W.; Chen, Y.-J.; Schlegel, H. B.; Endicott, J. F. *Inorg. Chem.* **2011**.
(28) Becke, A. D. *J. Chem. Phys.* **1993**, *98*, 5648.
(29) Hay, P. J.; Wadt, W. R. *J. Chem. Phys.* **1985**, *82*, 270.
(30) Wadt, W. R.; Hay, P. J. *J. Chem. Phys.* **1985**, *82*, 284.
(31) Frisch, M. J. T.; Schlegel, H. B.; Scuseria, G. E.; Robb, M. A.; Cheeseman, J. R.; Montgomery, J. A.; Vreven, T., Jr.; Kudin, K. N.; Burant, J. C.; Millam, J. M.; Iyengar, S. S.; Tomasi, J.; Barone, V.;

Mennucci, B.; Cossi, M.; Scalmani, G.; Rega, N.; Petersson, G. A.; Nakatsuji, H.; Hada, M.; Ehara, M.; Toyota, K.; Fukuda, R.; Hasegawa, J.; Ishida, M.; Nakajima, T.; Honda, Y.; Kitao, O.; Nakai, H.; Klene, M.; Li, X.; Knox, J. E.; Hratchian, H. P.; Cross, J. B.; Bakken, V.; Adamo, C.; Jaramillo, J.; Gomperts, R.; Stratmann, R. E.; Yazyev, O.; Austin, A. J.; Cammi, R.; Pomelli, C.; Ochterski, J.; Ayala, P. Y.; Morokuma, K.; Voth, G. A.; Salvador, P.; Dannenberg, J. J.; Zakrzewski, V. G.; Dapprich, S.; Daniels, A. D.; Strain, M. C.; Farkas, O.; Malick, D. K.; Rabuck, A. D.; Raghavachari, K.; Foresman, J. B.; Ortiz, J. V.; Cui, Q.; Baboul, A. G.; Clifford, S.; Cioslowski, J.; Stefanov, B. B.; Liu, G.; Liashenko, A.; Piskorz, P.; Komaromi, I.; Martin, R. L.; Fox, D. J.; Keith, T.; Al-Laham, M. A.; Peng, C. Y.; Nanayakkara, A.; Challacombe, M.; Gill, P. M. W.; Johnson, B. G.; Chen, W.; Wong, M. W.; Gonzalez, C.; Pople, J. A. *Gaussian 03*, Revision E.01; Gaussian Inc.: Wallingford, CT, 2004.

(32) *GaussView*; Gaussian Inc.: Wallingford, CT.

(33) Bignozzi, C. A.; Roffia, S.; Scandola, F. *J. Am. Chem. Soc.* **1985**, *107*, 1644.

(34) Macatangay, A. V. Ph.D. Dissertation, Wayne State University, Detroit, MI, 1999.

(35) Macatangay, A. V.; Endicott, J. F. *Inorg. Chem.* **2000**, *39*, 437.

(36) Macatangay, A. V.; Song, X.; Endicott, J. F. *J. Phys. Chem. A* **1998**, *102*, 7537.

(37) Richardson, D. E.; Taube, H. *Coord. Chem. Rev.* **1984**, *60*, 107.

(38) See the Supporting Information.

(39) Cohen, A. J.; Mori-Sanchez, P.; Yang, W. *Science* **2008**, *321*, 792.

(40) Mulliken, R. S.; Person, W. B. *Molecular Complexes*; Wiley-Interscience: New York, 1967.

(41) Kaim, W.; Klein, A.; Glockle, M. *Acc. Chem. Res.* **2000**, *33*, 755.

(42) Bossert, J.; Daniel, C. *Coord. Chem. Rev.* **2008**, *252*, 2493.

(43) Allard, M. M.; Odongo, O. S.; Lee, M. M.; Chen, Y.-J.; Endicott, J. F.; Schlegel, H. B. *Inorg. Chem.* **2010**, *49*, 6840.

(44) McConnell, H. M. *J. Chem. Phys.* **1961**, *35*, 508.

(45) *PSI-Plot*; Polysoftware International: Pearl River, NY.